as supplied by the STM supplier. Crystals of $SnSe_2$ and SnS_2 were grown with a Bridgman technique. All the other materials (including some $SnSe_2$) were grown via chemical vapor transport reactions in sealed quartz ampoules with only small variations on published procedures.[32]

(32) Preparation and Crystal Growth of Materials with Layered Structures. In *Physics and Chemistry of Materials with Layered Structures*; Lieth, R. M., Ed.; D. Reidel: Dordrecht, Holland, 1977; Vol. 1.

The crystal samples were mounted to copper disks with Ag epoxy and cleaved via sticky tape before each STM experiment.

Acknowledgment. The experimental assistance of Sue Riggs for STM operation and graphics and R. Scott McLean for assistance in crystal growth is gratefully acknowledged as are many helpful discussions with my colleagues and helpful suggestions of the reviewers.

A Photoelectron–Photoion Coincidence Study of $Fe(CO)_5$

K. Norwood,† A. Ali, G. D. Flesch, and C. Y. Ng*

Contribution from the Ames Laboratory,‡ U.S. Department of Energy, and Department of Chemistry, Iowa State University, Ames, Iowa 50011. *Received March 23, 1990. Revised Manuscript Received June 4, 1990*

Abstract: The photoelectron–photoion coincidence (PEPICO) spectra for $Fe(CO)_n^+$, $n = 0$–5, resulting from the photoionization of $Fe(CO)_5$ have been measured in the wavelength region of 650–1600 Å. The photoionization efficiency and PEPICO measurements provide new values for the ionization energy for $Fe(CO)_5$ and appearance energies for the formation of $Fe(CO)_n^+$, $n = 0$–4. These new values in turn yield values of 17.8 ± 0.9, 25.2 ± 1.1, 25.7 ± 1.4, 41.5 ± 1.6, and 39.3 ± 2.0 kcal/mol for the bond dissociation energies of $CO–Fe(CO)_n^+$, $n = 4$, 3, 2, 1, and 0, respectively. The collision-induced dissociation process, $FeCO^+ + Ar \rightarrow Fe^+ + CO + Ar$, has also been examined as a function of the collision energy and photoionization wavelength used in the preparation of reactant $FeCO^+$. The values for the dissociation energy of $Fe^+–CO$ determined by collision-induced dissociation and by photoionization are in agreement. Similar to the conclusion of the previous PEPICO study of $Cr(CO)_6^+$, the PEPICO data for $Fe(CO)_n^+$, $n = 0$–5, are consistent with a mechanism invoking the sequential fragmentation of CO, except for $Fe(CO)_2^+$, the data of which are in accord with the interpretation that $Fe(CO)_2^+$ may dissociate directly to both $FeCO^+$ and Fe^+.

I. Introduction

Accurate knowledge of the thermochemistry of organometallic compounds is fundamental to the understanding of their bondings and reactivities. The attempt to obtain detailed correlation of thermochemistry and reactivity in simple metal carbonyl ions represents an important goal of modern research in gaseous organometallic ion chemistry.[1,2] Transition-metal carbonyl compounds have been used in many industrial processes such as the vapor deposition of metal films[3] and the catalysis of organic reactions.[4-7] The desire to understand the reaction mechanisms involving intermediate organometallic radicals in these industrial processes has also been the impetus for detailed photochemical studies[8-13] and accurate thermochemical measurements[2,14] of these compounds.

The mass spectrometric technique is a well-established method for measuring the bond dissociation energies of organometallic ions.[15] Many electron impact experiments on $Fe(CO)_5$ have been reported previously.[16-20] These studies provide estimates for the bond dissociation energies of $CO–Fe(CO)_n^+$, $n = 0$–4. The energy resolution used in a photoionization experiment can be significantly superior to that achieved in an electron impact study. A photoionization efficiency study of the processes

$$Fe(CO)_5 + h\nu \rightarrow Fe(CO)_5^+ + e^- \quad (1)$$

$$\rightarrow Fe(CO)_4^+ + CO + e^- \quad (2)$$

$$\rightarrow Fe(CO)_3^+ + 2CO + e^- \quad (3)$$

$$\rightarrow Fe(CO)_2^+ + 3CO + e^- \quad (4)$$

$$\rightarrow FeCO^+ + 4CO + e^- \quad (5)$$

$$\rightarrow Fe^+ + 5CO + e^- \quad (6)$$

has been made.[21] The adiabatic ionization energy (IE) of $Fe(CO)_5$ has also been estimated previously in a photoionization experiment without mass selection.[22] The estimated value for the bond dissociation energy of $Fe^+–CO$ based on the assigned appearance energies (AE) for processes 5 and 6 disagrees with the results of electron impact experiments as well as those of the more recent photodissociation[23] and ligand displacement studies.[24] The photoionization efficiency (PIE) spectra for $Fe(CO)_5^+$ and

† Catron Research Fellow.

‡ Operated for the U.S. Department of Energy by Iowa State University under Contract No. W-7405-Eng-82. This work was supported by the Director for Energy Research, Office of Basic Energy Sciences.

(1) Foster, M. S.; Beauchamp, J. L. *J. Am. Chem. Soc.* **1975**, *97*, 4808.
(2) Connor, J. A. *Curr. Top. Chem.* **1977**, *71*, 71.
(3) Clements, P. J.; Sale, F. R. *Metall. Trans.* **1976**, *7B*, 435.
(4) Bradford, C. W. *Platinum Met. Rev.* **1972**, *16*, 50.
(5) Howe, R. F.; Davidson, D. E.; Whan, D. A. *J. Chem. Soc. Trans. I* **1972**, *68*, 2266.
(6) Howe, R. F. *Inorg. Chem.* **1976**, *15*, 486.
(7) Brenner, A.; Burwell, R. L., Jr. *J. Am. Chem. Soc.* **1975**, *97*, 2565.
(8) Wrighton, M. *Chem. Rev.* **1974**, *74*, 401.
(9) Lewis, K. E.; Golden, D. M.; Smith, G. P. *J. Am. Chem. Soc.* **1984**, *106*, 3905.
(10) Yardley, J. T.; Gitlin, B.; Nathanson, G.; Rosan, A. M. *J. Chem. Phys.* **1981**, *74*, 361, 370.
(11) Ouderkirk, A. J.; Wermer, P.; Schultz, N. L.; Weitz, E. *J. Am. Chem. Soc.* **1983**, *105*, 3354.
(12) Ouderkirk, A. J.; Weitz, E. *J. Chem. Phys.* **1983**, *79*, 1089.
(13) Kotzian, M.; Rosch, N.; Schroder, H.; Zerner, M. C. *J. Am. Chem. Soc.* **1989**, *111*, 7687.
(14) Behrens, R. G. *J. Less-Common Met.* **1977**, *56*, 55.
(15) Litzow, M. R.; Spalding, T. R. *Mass Spectrometry of Inorganic and Organometallic Compounds*; Elsevier: Amsterdam, 1973.
(16) Bidinosti, D. R.; McIntyre, N. S. *Can. J. Chem.* **1967**, *45*, 641.
(17) Foffani, A.; Pignataro, S.; Cantone, B.; Grasso, F. *Z. Physik. Chem.* **1965**, *45*, 79.
(18) Junk, G. A.; Svec, H. J. *Z. Naturforsch.* **1968**, *23B*, 1.
(19) Winters, R. E.; Kiser, R. W. *Inorg. Chem.* **1964**, *3*, 699.
(20) Clements, P. J.; Sale, F. R. *Metall. Trans.* **1976**, *7B*, 171.
(21) Distefano, G. *J. Res. Natl. Bur. Stand.* **1970**, *74A*, 233.
(22) Lloyd, D. R.; Schlag, E. W. *Inorg. Chem.* **1969**, *8*, 2544.
(23) Cassady, C. J.; Freiser, B. S. *J. Am. Chem. Soc.* **1984**, *106*, 6176.
(24) Foster, M. S.; Beauchamp, J. L. *J. Am. Chem. Soc.* **1975**, *97*, 4808.

0002-7863/90/1512-7502$02.50/0

$Fe(CO)_4^+$ obtained previously by Distefano[21] reveal significant autoionization features. This observation is surprising in view of the expected facile dissociation of excited $Fe(CO)_5^+$ and $Fe(CO)_5$ formed in the vacuum ultraviolet region.

Because of the scattered light effect of the diffraction grating, the intensity of a specific ion observed in a photoionization experiment remains finite even though the monochromator is set at a photon energy below the IE or AE for its formation. This, together with the hot band effect, makes the determination of the true AE difficult. In this article, we present a photoelectron–photoion coincidence (PEPICO) study of $Fe(CO)_5$. By using the supersonic molecular beam method to introduce $Fe(CO)_5$ into the photoionization region, we hope to reduce the rotational and low-frequency vibrational hot bands effect on the measured AEs for processes 1–6.[25] We have pointed out previously[26] that employing the PEPICO method can significantly reduce the scattered light effect because photoelectrons (PE) produced by scattered light are expected to have kinetic energies different from the accepting energy band width set by the electron energy analyzer.

In addition to information about the AEs for processes 1–6, the PEPICO spectra for $Fe(CO)_n^+$, n = 0–5, obtained in this experiment also shed light on the unimolecular dissociation routes for these ions. A similar PEPICO study of $Cr(CO)_6$ using the gas cell method has been reported by Meisels and co-workers.[27]

We have also examined the threshold for the collision-induced dissociation process

$$FeCO^+ + Ar \rightarrow Fe^+ + CO + Ar \qquad (7)$$

in which $FeCO^+$ is formed by the dissociative ionization process. This experiment demonstrates that the cross section for process 7 depends strongly on the internal excitation of $FeCO^+$.

II. Experimental Section

A. Measurements of the PIE, PE, and PEPICO Spectra for $Fe(CO)_n^+$, n = 0–5. The experimental arrangement of the PEPICO apparatus used in these measurements has been described in detail previously.[28-30] Briefly, the apparatus consists of a 3 m near normal incidence vacuum ultraviolet (VUV) monochromator, a capillary discharge lamp, a tungsten photoelectric VUV light detector, a molecular beam source, a quadrupole mass spectrometer (QMS) for ion detection, and an electron energy analyzer for threshold photoelectron (TPE) detection.

The grating employed in this study is a Bausch and Lomb 1200 lines/mm Os coated aluminum grating blazed at 1360 Å. Either the hydrogen many-lined pseudocontinuum or the helium Hopfield continuum is used as the light source, depending on the wavelength region desired.

The iron pentacarbonyl is obtained from Alfa Products with a stated purity of 98%. In this experiment, a continuous $Fe(CO)_5$ beam seeded in Ar is produced by supersonic expansion through a stainless steel nozzle with a nozzle diameter of 125 μm at a total stagnation pressure of about 450 Torr. The partial pressure of $Fe(CO)_5$ is estimated to be approximately 30 Torr, which is determined by the vapor pressure of the liquid sample maintained at 298 K. In order to avoid condensation at the nozzle, the nozzle is warmed by a heater and maintained at a temperature slightly above the room temperature. The molecular beam is collimated by a conical skimmer before entering the photoionization chamber. During the experiment, the photoionization chamber is maintained at $\leq 2 \times 10^{-5}$ Torr.

A differential pulsed PIPECO scheme[30] is used for coincidence measurements. The coincidence detection cycle is initiated by an electronic pulse signifying the arrival of a TPE at the electron detector. The electronic pulse triggers two identical extraction pulses, which have a width of 80 ns and a height of 120 V, to extract photoions toward the ion detector. The QMS is used to select the ion of interest for detection. The first and second extraction pulses are delayed by 0 and 40 μs, respectively, with respect to the triggering electronic pulse. The electron flight time from the photoionization region to the electron detector is ≤0.1 μs. In such a short time, the correlated photoion is expected to remain in the photoionization region. Thus, the first extraction pulse serves to extract the correlated photoion as well as background ions, while the second extraction pulse draws out only background ions. The photoionization region is maintained nearly field free, except during the application of the ion extraction pulse. A potential barrier is used between the photoionization region and the entrance of the QMS such that no ions are transmitted to the ion detector without the application of the extraction pulse. The ions arriving at the ion detector are recorded by using a multichannel scaler. The difference of the ion intensities detected due to the first and second extraction pulses represents the true coincidence signal. The coincidence cycle is completed in a period of 100 μs. The first TPE electronic pulse generated by the electron detector after this period initiates a new coincidence cycle.

All data are obtained with an optical resolution of 1.5 Å [full width at half maximum (FWHM)]. The wavelength interval used varies in the range of 1–5 Å. The counting at each data point ranges from 30 to 200 s.

B. Collision-Induced Dissociation of $FeCO^+$. The triple-quadrupole double-octopole photoionization apparatus used in this study has been described previously.[31-33] It consists of a 0.2-m VUV monochromator, a discharge lamp, a tungsten VUV light detector, three QMSs, two radio frequency (rf) octopole ion guide reaction gas cells, a supersonic free jet production system, and a scintillation ion detector.

The experimental procedures for the measurement of absolute total cross sections are similar to those outlined previously.[33] Here, $FeCO^+$ reactant ions are produced by the dissociative photoionization of $Fe(CO)_5$ in a free jet at 790 and 906 Å by using a wavelength resolution of 3.5 Å (FWHM). The $Fe(CO)_5$ free jet seeded in He is produced by supersonic expansion through a 5-μm diameter quartz nozzle at a total stagnation pressure of 150 Torr. The ratio for the pressure of He to that of $Fe(CO)_5$ is about 5. Under these expansion conditions, the photoionization chamber maintains a pressure of 2×10^{-5} Torr. The reactant $FeCO^+$ ions formed in the photoionization region are extracted perpendicular to the free jet and selected by the reactant QMS before colliding with Ar in the upper rf octopole ion guide reaction gas cell. The Ar gas cell pressure is monitored with a Baratron manometer (MKS Model 390HASP05), and an Ar gas cell pressure of 2×10^{-4} Torr is used in this experiment. The $FeCO^+$ reactant ions and Fe^+ product ions are mass selected by the product QMS and detected by the scintillation ion detector. The lower rf octopole ion guide and middle QMS are used in this experiment as ion lenses to transmit all ions.

The $FeCO^+$ reactant laboratory ion beam energy (E_{lab}) is measured by the retarding potential energy method. At each E_{lab}, the product Fe^+ collection efficiency is maximized carefully by optimizing the rf voltage applied to the upper rf octopole ion guide and the transmission of the ion lenses and product QMS. The uncertainties for absolute cross sections reported are estimated to be less than 25%.

III. Results and Discussion

A. PIE Spectra for $Fe(CO)_n^+$, n = 0–5. The PIE spectra for $Fe(CO)_n^+$, n = 0–5, are shown in Figures 1a–c and 2a–c. The structures of all the PIE spectra, except that of the Fe^+ spectrum, observed here are different from those obtained previously.[21] The rich autoionization features found in the PIE spectra for $Fe(CO)_5^+$ and $Fe(CO)_4^+$ by Distefano are not discernible in the spectra shown in Figure 1a,b. Minor oscillations of the PIE for $Fe(CO)_5^+$ observed in the region from 1000–1550 Å are believed to be caused by the light modulation effect of the hydrogen many-lined pseudocontinuum. The PIE spectra for $Fe(CO)_n^+$, n = 3–5, exhibit two broad peaks at approximately 890 and 990 Å. The decreases of PIEs for $Fe(CO)_n^+$, n = 3–5, as the photon energy is increased from 14.17 (875 Å) to 16.53 eV (750) correspond to the increases of PIEs for $FeCO^+$ and Fe^+. Other than minor structure observed in the PIE spectrum for $FeCO^+$, both the PIE spectra for Fe^+ and $FeCO^+$ are found to increase monotonically with increasing photon energy. The lack of autoionization structure in the PIE spectra for $Fe(CO)_n^+$, n = 0–5, is consistent with the expectation that excited $Fe(CO)_5$ and $Fe(CO)_5^+$, formed by photoexcitation and photoionization, respectively, dissociate rapidly in the wavelength region of interest here.

It is interesting to compare the PIE spectra for $Fe(CO)_n^+$, n = 0–5, with the PE spectrum of $Fe(CO)_5$. The HeI PE spectrum

(25) Ng, C. Y. *Adv. Chem. Phys.* **1983**, *52*, 265.
(26) Norwood, K.; Guo, J.-H.; Luo, G.; Ng, C. Y. *J. Chem. Phys.* **1989**, *90*, 6026.
(27) Das, P. R.; Nishimura, T.; Meisels, G. G. *J. Phys. Chem.* **1985**, *89*, 2808.
(28) Norwood, K.; Guo, J.-H.; Luo, G.; Ng, C. Y. *Chem. Phys.* **1989**, *129*, 109.
(29) Norwood, K.; Guo, J.-H.; Ng, C. Y. *J. Chem. Phys.* **1989**, *90*, 2995.
(30) Norwood, K.; Ng, C. Y. *Chem. Phys. Lett.* **1989**, *156*, 145.
(31) Liao, C.-L.; Shao, J.-D.; Xu, R.; Flesch, G. D.; Li, Y.-G.; Ng, C. Y. *J. Chem. Phys.* **1986**, *85*, 3874.
(32) Shao, J.-D.; Li, Y.-G.; Flesch, G. D.; Ng, C. Y. *J. Chem. Phys.* **1987**, *86*, 170.
(33) Shao, J.-D.; Ng, C. Y. *J. Chem. Phys.* **1986**, *84*, 4317.

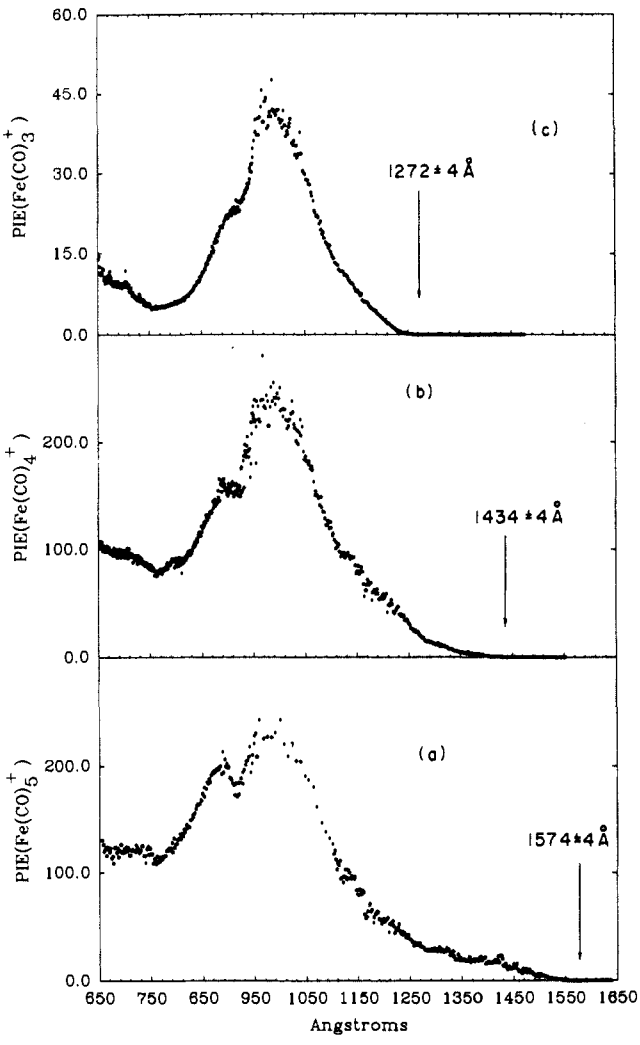

Figure 1. PIE spectra in the wavelength region of 650–1650 Å: (a) $Fe(CO)_5^+$, (b) $Fe(CO)_4^+$, and (c) $Fe(CO)_3^+$.

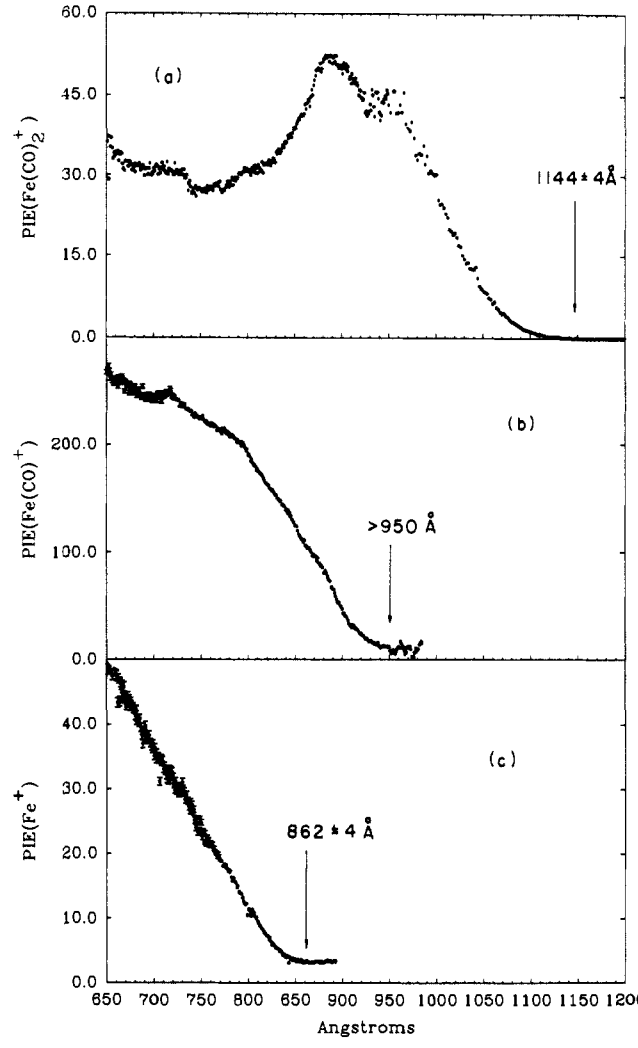

Figure 2. PIE spectra in the wavelength region of 650–1200 Å: (a) $Fe(CO)_2^+$, (b) $FeCO^+$, and (c) Fe^+.

for $Fe(CO)_5$ reported previously[34] is reproduced in Figure 3. The discontinuity in the PE spectrum at about 13 eV is due to the change in the PE count scale. The first two PE peaks centered at 8.6 and 9.9 eV arise from the ejection of an electron from the 10e′ and 3e″ orbitals, respectively.[13,34] According to the electron population analysis, the 10e′ and 3e″ orbitals have mainly the Fe(3d) character. The PE peaks observed at ionization energies higher than 13.5 eV are assigned to electronic states corresponding to the removal of electrons from the 5σ and 1π orbitals of the CO ligands. The lower intensities observed for the PE peaks at 8.6 and 9.9 eV compared to those at ionization energy above 13.5 eV may be rationalized by the fact that the Fe(3d) orbitals are shielded by the CO ligands. The energy thresholds for the formation of $Fe(CO)_n^+$, n = 0–5, from processes 1–6 are indicated in Figure 3. The thresholds for the formation of $Fe(CO)_4^+$ and $Fe(CO)_3^+$ approximately coincide with the 10e′ and 3e″ PE peaks, respectively. The significant increases in PIE for $Fe(CO)_n^+$, n = 3–5, as photon energy is increased in the range of 11.3–13 eV (950–1100 Å) can be attributed to the formation of $Fe(CO)_5^+$ in electronic excited states corresponding to the removal of electrons from the orbitals of CO. Similarly, the observed increases in PIEs for $Fe(CO)_n^+$, n = 0–5, at wavelengths shorter than 750 Å (16.5 eV) may also be due to the population of new electronic states of $Fe(CO)_5^+$. We note that the structures observed in the PIE spectra may also be due to autoionization states of $Fe(CO)_5$.

The AEs for the formation of $Fe(CO)_n^+$, n = 0–5, from processes 1–6, determined by the PIE spectra, are compared in Table

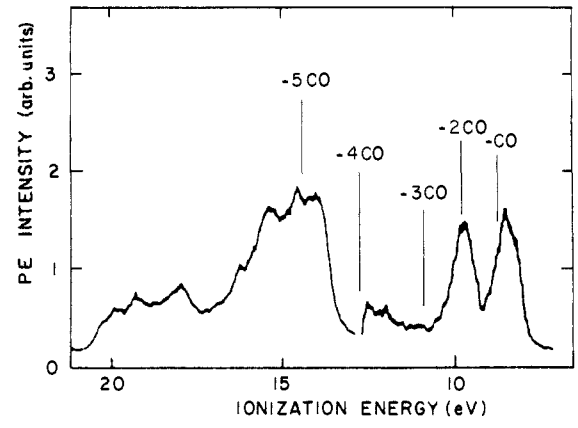

Figure 3. HeI PE spectrum of $Fe(CO)_5$ obtained by Baerends et al (ref 34). The break at the ionization energy of ≈13 eV is due to the change in scale of electron-counting rate.

I to those obtained in the previous photoionization studies.[21,22] The adiabatic IE for $Fe(CO)_5$ determined here is lower by about 0.1 eV[21] than those reported previously. The AEs for $Fe(CO)_3^+$ and $Fe(CO)_4^+$ are also found to be slightly lower than those obtained by Distefano. Contrary to the trends observed for $Fe(CO)_n^+$, n = 3–5, the AEs for $Fe(CO)_n^+$, n = 0–2, obtained in this experiment are higher than the results of the previous photoionization study.[21] In the cases of $FeCO^+$ and Fe^+, the differences between the AEs of the two experiments are significant. Due to the low PIEs for $FeCO^+$ and strong atomic resonance lines superimposed in the helium Hopfield continuum, the PIE spectrum for $FeCO^+$ in the

(34) Baerends, E. J.; Oudshoorn, Ch.; Oskam, A. *J. Electron Spectrosc. Relat. Phenom.* **1975**, *6*, 259.

Table I. Appearance Energies for the Formation of $Fe(CO)_n^+$ Determined by the PIE and PEPICO Spectra for $Fe(CO)_n^+$, $n = 0–5$

ions	appearance energies (eV) PIE	PEPICO[a]
$Fe(CO)_5^+$	7.877 ± 0.020 (1574 ± 4 Å)[a] 7.98 ± 0.01 (1554 Å)[b] 7.96 ± 0.02[c]	7.897 ± 0.025 (1570 ± 5 Å)
$Fe(CO)_4^+$	8.646 ± 0.024 (1434 ± 4 Å)[a] 8.77 ± 0.10 (1413 Å)[b]	8.670 ± 0.030 (1430 ± 5 Å)
$Fe(CO)_3^+$	9.747 ± 0.031 (1272 ± 4 Å)[a] 9.87 ± 0.10 (1256 Å)[b]	9.763 ± 0.038 (1270 ± 5 Å)
$Fe(CO)_2^+$	10.838 ± 0.038 (1144 ± 4 Å)[a] 10.68 ± 0.10 (1159 Å)[b]	10.876 ± 0.048 (1140 ± 5 Å)
$FeCO^+$	<13.05 (>950 Å)[a] 1153 ± 0.10 (1075 Å)[b]	12.677 ± 0.052 (978 ± 4 Å)
Fe^+	14.383 ± 0.067 (862 ± 4 Å)[a] 14.03 ± 0.10 (884 Å)[b]	14.383 ± 0.067 (862 ± 4 Å)

[a] This work. [b] Reference 21. [c] Reference 22.

wavelength region >950 Å suffers from light modulation effects, making the AE measurement for $FeCO^+$ difficult. The AE value for $FeCO^+$ estimated by the PIE spectrum represents an upper limit.

B. PEPICO Spectra for $Fe(CO)_n^+$, $n = 0–5$. The PEPICO spectra for $Fe(CO)_n^+$, $n = 0–5$, are depicted in Figures 4a–c and 5a–c. The TPE spectrum for $Fe(CO)_5$ in the wavelength region of 650–950 Å measured in this experiment is shown in Figure 5d for comparison. The structure of the TPE spectrum is in agreement with that resolved in the HeI PE spectrum shown in Figure 3.

The general profiles for the PEPICO spectra for $Fe(CO)_n^+$, $n = 1–5$, are similar, exhibiting a broad peak structure. The main peak observed in the PEPICO spectra for $Fe(CO)_5^+$ coincides with the 10e′ PE peak, while those for $Fe(CO)_4^+$ and $Fe(CO)_3^+$ match the 3e″ PE peak resolved in the HeI PE spectrum. The PEPICO intensity for $Fe(CO)_5^+$ drops sharply as the photon energy is increased above the AE for $Fe(CO)_4^+$. At wavelengths shorter than 1405 Å, the PEPICO intensities for $Fe(CO)_5^+$ are essentially zero, indicating that, within the ≤100-μs time scale of this experiment, complete dissociation of $Fe(CO)_5^+$ into $Fe(CO)_4^+$ is realized when $Fe(CO)_5^+$ is formed with internal energies $[h\nu - IE(Fe(CO)_5)] \geq 0.95$ eV. In the $Fe(CO)_5^+$ internal energy range of approximately 2.59–2.96 eV (1144–1185 Å), $Fe(CO)_5^+$ may dissociate completely into $Fe(CO)_3^+ + 2CO$ via a direct or a two-step mechanism involving the $Fe(CO)_4^+$ intermediate. The PEPICO spectra for $Fe(CO)_n^+$, $n = 0–5$, supports the conclusion that if the internal energy for $Fe(CO)_5^+$ is increased continuously from 0–6.5 eV (862–1574 Å), the dissociation of $Fe(CO)_5^+$ may follow a sequential pathway

$$Fe(CO)_5^+ \xrightarrow{-CO} Fe(CO)_4^+ \xrightarrow{-CO} Fe(CO)_3^+ \xrightarrow{-CO} Fe(CO)_2^+ \xrightarrow{-CO} FeCO^+ \xrightarrow{-CO} Fe^+ \quad (8)$$

losing one CO ligand at a time. The sequential CO elimination mechanism for $Fe(CO)_5^+$ is consistent with the proposed dissociation model for photoexcited $Fe(CO)_5$.[35,36] In the recent laser photofragmentation studies of $Fe(CO)_5$, Waller and Hepburn[35] and Venkataraman et al.[36] show that the kinetic energy distributions of photofragments resulting from the dissociation of photoexcited $Fe(CO)_5$ are consistent with statistical models in which complete energy randomization is achieved prior to sequential CO ligand eliminations.

In the wavelength region of 750–862 Å, which corresponds to the internal energy range of 6.51–8.65 eV for $Fe(CO)_5^+$, the PEPICO intensities for $Fe(CO)_2^+$, $FeCO^+$, and Fe^+ are finite. This observation is in accord with the interpretation that $Fe(CO)_2^+$ may dissociate directly to both $FeCO^+$ and Fe^+. At $Fe(CO)_5^+$ internal energies greater than 9.1 eV (730 Å), Fe^+ becomes essentially the only product ion. We have not measured carefully the relative PEPICO intensities for $Fe(CO)_2^+$, $FeCO^+$, and Fe^+.

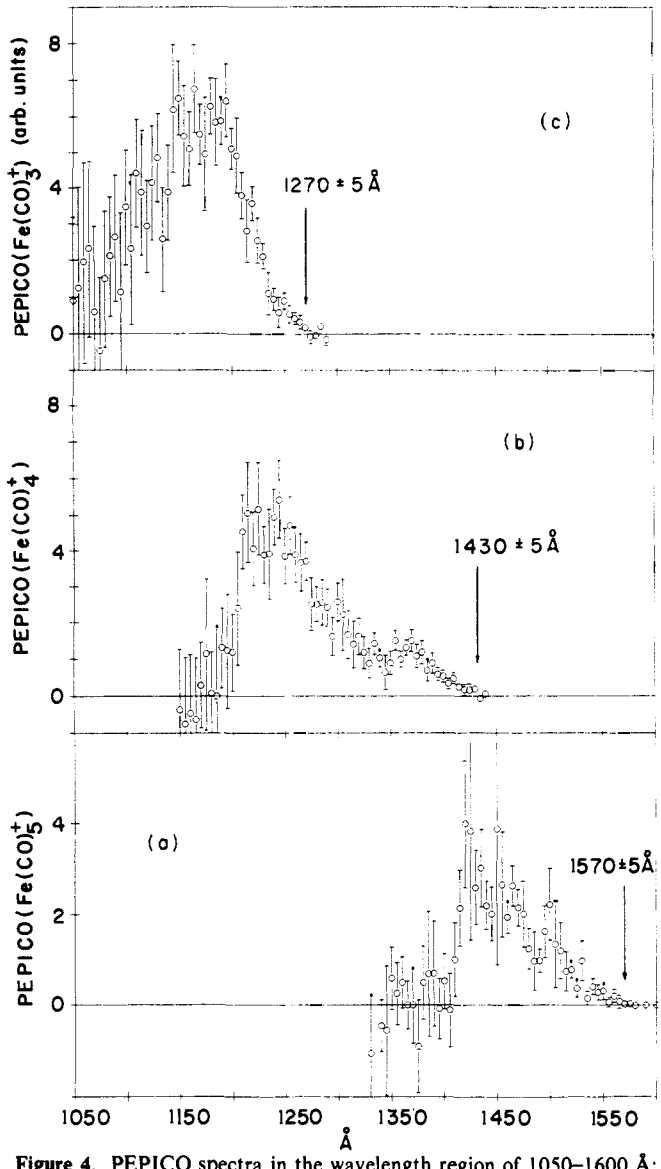

Figure 4. PEPICO spectra in the wavelength region of 1050–1600 Å: (a) $Fe(CO)_5^+$, (b) $Fe(CO)_4^+$, and (c) $Fe(CO)_3^+$. All PEPICO spectra have been normalized by the light intensity.

However, the relative PEPICO intensities for these ions can be estimated because the sum of their intensities should yield a spectrum identical with the TPE spectrum shown in Figure 5d.

The routes identified for the unimolecular decomposition of energy-selected $Fe(CO)_5^+$ are similar to those found for $Cr(CO)_6^+$.[27] In the PEPICO study of $Cr(CO)_6$, Meisels and coworkers conclude that successive loss of CO ligand is the dissociation route except for $Cr(CO)_2^+$, which appears to fragment directly to both $CrCO^+$ and Cr^+.

The IE for $Fe(CO)_5^+$ and the AEs for $Fe(CO)_n^+$, $n = 0–4$, determined by the PEPICO spectra of these ions are summarized in Table I. Below the assigned thresholds for these ions, the PEPICO intensities for the corresponding ions are essentially zero, confirming the expectation that the scattered light effect is substantially suppressed in a PEPICO experiment. With the exception of the AE for $FeCO^+$, which is found to be lower than that estimated by the $FeCO^+$ PIE spectrum, all AE values determined by the PIE and PEPICO measurements are in good agreement. The uncertainties for the IE and AEs given in Table I represent the reproducibilities of the measurements.

C. Thermochemistry for $Fe(CO)_n^+$, $n = 0–5$, and $Fe(CO)_5$. By using the IE for $Fe(CO)_5$ and AEs for $Fe(CO)_n^+$, $n = 0–5$, determined in this experiment, the bond dissociation energies for $CO–Fe(CO)_n^+$, $n = 0–4$, are calculated and listed in Table II. The values for the bond dissociation energies estimated in the previous photoionization and photodissociation studies[21,37] and the

(35) Waller, I. M.; Hepburn, J. W. *J. Chem. Phys.* **1988**, *88*, 6658.
(36) Venkataraman, B. K.; Bandukwalla, G.; Zhang, Z.; Vernon, M. *J. Chem. Phys.* **1989**, *90*, 5510.

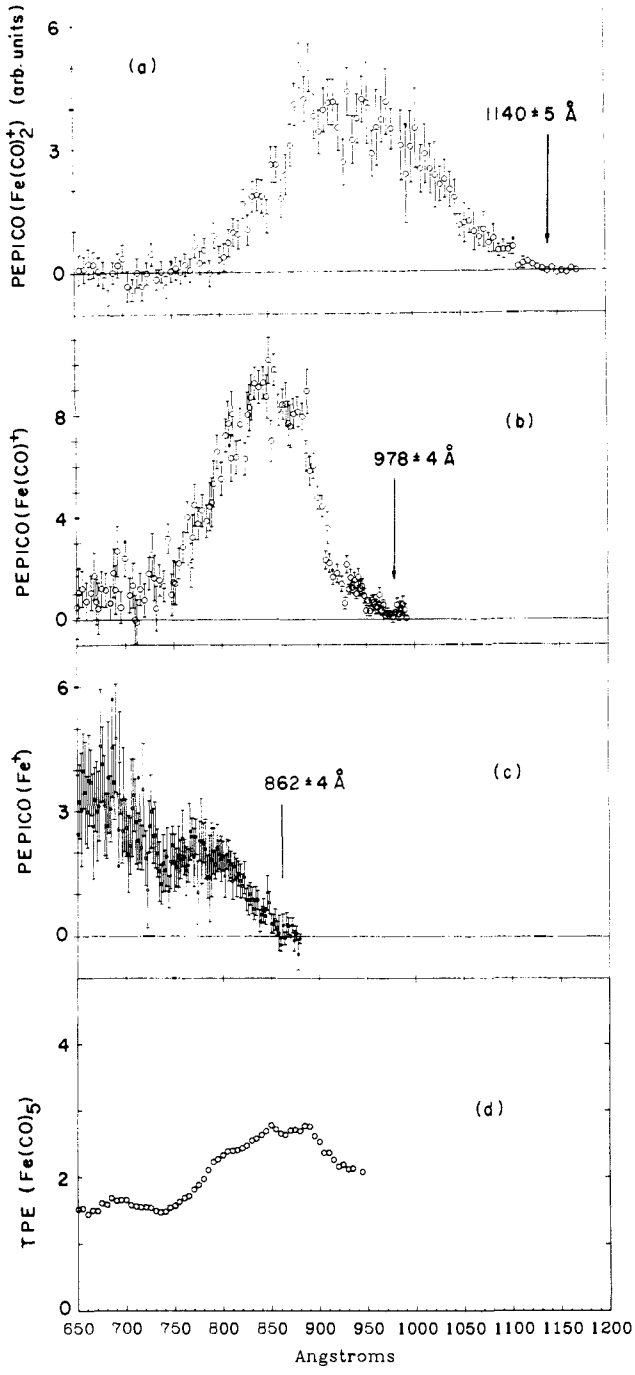

Figure 5. PEPICO and TPE spectra in the wavelength region of 650–1200 Å: (a) PEPICO spectrum for $Fe(CO)_2^+$, (b) PEPICO spectrum for $FeCO^+$, (c) PEPICO spectrum for Fe^+, and (d) TPE spectrum for $Fe(CO)_5$. All PEPICO and TPE spectra have been normalized by the light intensity.

recent theoretical calculation[38] are also included in the table. The error limits for the D_0 values given in Table II represent the reproducibilities of the threshold measurements.

Due to the cooling effect of the supersonic expansion, we assume that the values obtained here correspond to bond dissociation energies at 0 K (D_0). Iron pentacarbonyl possesses several soft bending modes with frequencies in the range of 75–100 cm^{-1},[39,40] Since the expansion conditions for the $Fe(CO)_5$ beam used are relatively mild, complete relaxation for low-frequency vibrational populations of $Fe(CO)_5$ at room temperature probably are not achieved. It is difficult to assess the corrections for the vibrational hot band effect on the IE and AEs determined in this experiment. However, we note that the bond dissociation energies depend on the differences of the thresholds for the formations of $Fe(CO)_n^+$, $n = 0$–5. The vibrational hot band effect on the bond dissociation energies should not be significant provided that a consistent method is used to determined the thresholds. A detailed discussion about possible difficulties, such as the hot band and kinetic shift effects, in the determination of true AEs from PIE measurements can be found in ref 41.

Although the values for the bond dissociation energies of CO–$Fe(CO)_n^+$, $n = 3$ and 4, reported by Distefano[21] are in agreement with the corresponding D_0 values obtained in this experiment, we note that the bond dissociation energies of CO–$Fe(CO)_n^+$, $n =$ 0–4, estimated in the previous photoionization study[21] correspond to values at room temperature. The D_0 value of 39.3 ± 2.0 kcal/mol determined for Fe^+–CO is consistent with the upper bounds obtained in the photodissociation studies.[23,37]

Recently, a high level ab initio calculation[38] has been carried out for the iron mono- and dicarbonyl cations. This calculation predicts that the D_e values for CO-Fe^+ and CO-$FeCO^+$ are 30.3 (36.1) and 34.5 (34.5) kcal/mol, respectively. The values in parentheses represent asymptotic D_e values for the $Fe^+[d^7(^4F)]$ state. After correcting for the zero-point energies of −1.18 kcal/mol for $FeCO^+$ and −2.694 kcal/mol for $Fe(CO)_2^+$, the theoretical D_0 values for CO–Fe^+ and CO–$FeCO^+$ are 29.1 (34.9) and 33.1 (33.1) kcal/mol, respectively. Barnes et al.[38] indicate that the calculation underestimates the dissociation energy by ≈2–3 kcal/mol per ligand due to the basis set incompleteness and superposition errors. They also point out that in electron and photon impact experiments, the dissociation is likely to occur to the $Fe^+[3d^7(^4F)]$ asymptote. Thus, the comparison should be made with the values in the parentheses. After taking into account the error estimated in the calculation and the uncertainty of the experimental value, the experimental and theoretical D_0 values for Fe^+–CO are in agreement. However, the theoretical D_0 value for CO-$FeCO^+$ is slightly lower than that obtained in this experiment.

By using the AE of 14.38 ± 0.07 for process 6 and the IE of $Fe(CO)_5$ (7.877 ± 0.20 eV), we calculate an endothermicity of 149.9 ± 1.6 kcal/mol (6.50 ± 0.07 eV) for the dissociation process

$$Fe(CO)_5^+ \rightarrow Fe^+ + 5CO \qquad (9)$$

On the basis of the known values for the heats of formation for $Fe^+(\Delta H_{f0} = 280.4 \pm 0.4$ kcal/mol) and $CO(\Delta H_{f0} = -27.2$ kcal/mol),[41] we obtain a value of −5.5 ± 1.7 kcal/mol for $\Delta H_{f0}[Fe(CO)_5^+]$. The latter value, together with the IE for $Fe(CO)_5$, allows the calculation of a value of −187.1 ± 1.7 kcal/mol for $\Delta H_{f0}[Fe(CO)_5]$. The conversion of $\Delta H_{f0}[Fe(CO)_5]$ to $\Delta H_{f298}[Fe(CO)_5]$ requires corrections due to translation, rotational, and vibrational populations at 298 K, which are estimated to be 7.9 kcal/mol.[14] Therefore, we arrive at a value of −179.2 ± 1.7 kcal/mol for $\Delta H_{f298}[Fe(CO)_5]$. This value is in agreement with the literature value of $\Delta H_{f298}[Fe(CO)_5] = -175.2 \pm 3$ kcal/mol[14] after taking into account the experimental uncertainties. The agreement observed between the literature value for $\Delta H_{f298}[Fe(CO)_5]$ and that determined here indicates that the IE for $Fe(CO)_5$ and AE for process 6 obtained by the PIE and PEPICO measurements are reliable.

The value of −175.2 ± 3 kcal/mol[14] for $\Delta H_{f298}[Fe(CO)_5]$ is based on the average (−185.2 kcal/mol)[42] of the heats of combustion of −187.8 kcal/mol and −182.6 kcal/mol for $Fe(CO)_5$ (l) at 298.15 K reported by Mittasch[43,45] and Cotton, Kischer, and

(37) Tecklenberg, R. E.; Bricher, D. L.; Russell, D. H. *Organometallics* **1988**, *7*, 2506.
(38) Barnes, L. A.; Rosi, M.; Bauschlicher, C. W., Jr. *J. Chem. Phys.* In press.
(39) King, F. T.; Lippincott, E. R. *J. Am. Chem. Soc.* **1956**, *78*, 4192.
(40) Jones, L. H.; McDowell, R. S.; Goldbatt, M.; Swanson, B. I. *J. Chem. Phys.* **1972**, *57*, 2050.
(41) Rosenstock, H. M.; Draxl, K.; Steiner, B. W.; Herron, J. T. *J. Phys. Ref. Data 6, Suppl. 1* **1977**.
(42) Wagman, D. D.; Evans, W. H.; Parker, V. B.; Halow, I.; Bailey, S. M.; Schumm, R. H. *Selected Values of Chemical Thermodynamic Properties*, U.S. National Bureau of Standards Technical Note 270-3, January 1969; 270-4, May 1969.

Table II. Bond Dissociation Energies at 0 K (D_0) for $CO–Fe(CO)_{n-1}^+$ and $CO–Fe(CO)_{n-1}$, n = 1–5, and IE of $Fe(CO)_n$, n = 1–5

compounds	D_0 (kcal/mol) ionic	D_0 (kcal/mol) neutral	IE (eV)
$Fe(CO)_5$	17.8 ± 0.9[a]	39 ± 2[f]	7.897 ± 0.025[a]
	18.2[b]	41 ± 12[g]	
$Fe(CO)_4$	25.2 ± 1.1[a]	18 ± 9[g]	6.98 ± 0.09[i]
	25.4[b]	10[h]	≈6.9[j]
$Fe(CO)_3$	25.7 ± 1.4[a]	32 ± 7[g]	≈7.3[j]
	18.7[b]	25[h]	≈7.6[k]
$Fe(CO)_2$	41.5 ± 1.6[a]	23 ± 7[g]	≈7.0[j]
	19.6[b]	>27[h]	≈7.7[k]
	33.1 (33.1)[c]		
FeCO	39.3 ± 2.0[a]	23 ± 7[g]	≈7.9[j]
	57.7[b]	<39[h]	<8.4[k]
	29.1 (34.9)[c]		
	≤43 ± 3[d]		
	<78[e]		
av bond energy	29.9[a]		

[a] This work. [b] Reference 21. Values correspond to room temperature. [c] Reference 38. These are theoretical D_e values corrected for the zero point energies. The values in parentheses are asymptotic D_0 values for the $Fe^+(d^7)$ state. See text. [d] Reference 23. [e] Reference 37. [f] Reference 9. This D_0 value is converted from the bond dissociation energy at 298 K. [g] References 35 and 45. [h] Reference 36. [i] Value obtained by using the D_0 value for $CO–Fe(CO)_4$ of ref 9 and AE for process 2. [j] Values obtained by using estimated bond dissociation energies of refs 35 and 45 and AEs for processes 2–5. [k] Values obtained by using estimated bond dissociation energies of ref 36 and AEs for processes 2–5.

Wilkinson,[45] respectively. As we pointed out above, the IE for $Fe(CO)_5$ and AEs for $Fe(CO)_n^+$, n = 0–4, obtained in this experiment probably correspond to a vibrational temperature higher than 0 K. If this is the case, the AE for process 9 would yield a slightly lower value for $\Delta H_{f298}[Fe(CO)_5]$ compared to −179.2 kcal/mol and would favor the value of −187.8 kcal/mol for the heat of combustion of $Fe(CO)_5$ (l) at 298.15 K.

The average bond dissociation energy for the $Fe(CO)_5^+$ ion system is equal to D_+ = 29.9 kcal/mol. It has been shown that the average bond dissociation energy (D) for the neutral $Fe(CO)_5$ system and D_+ are related by the equation

$$IE[Fe(CO)_5] + 5D_+ = IE(Fe) + 5D \qquad (10)$$

Since the value for IE(Fe) (= 7.870 eV)[46] is nearly identical with that for $IE[Fe(CO)_5]$, we have $D \approx D_+$.

The bond dissociation energy for $CO–Fe(CO)_4$ at 298 K is determined to be 41 ± 2 kcal/mol.[9] Assuming that the vibrational excitations for $Fe(CO)_5$ and $Fe(CO)_4$ at 298 K are similar, we estimate that the endothermicity for process 11 at 0 K is D_0 = 39 ± 2 kcal/mol.

$$Fe(CO)_5 \rightarrow Fe(CO)_4 + CO \qquad (11)$$

According to molecular bonding schemes,[47,48] the bonding of transition-metal carbonyls can be considered to have two main contributions: the σ-type bonding resulting from the overlap of the lone-pair orbital on the C atom of CO and s, p, and $d(e_g)$ orbitals of the metal and the π-type bonding due to the interaction between the metal $d(t_{2g})$ orbital and the unoccupied π^* orbitals of the CO ligands. The removal of an electron from the 3d orbital of Fe is expected to strengthen the σ-type bonding and weaken the π-type interaction. The substantially lower D_0 value of 17.5 kcal/mol observed for $CO–Fe(CO)_4^+$ compared to that of 39 kcal/mol for $CO–Fe(CO)_4$ suggests that the loss of π-stabilization is far greater than the gain in σ-stabilization.

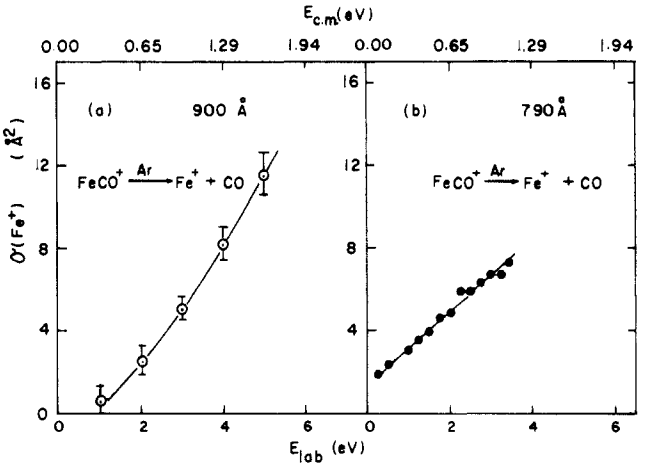

Figure 6. Collision-induced dissociation for $FeCO^+$ + Ar: (a) $FeCO^+$ formed at 900 Å and (b) $FeCO^+$ formed at 790 Å.

By using the thresholds for processes 2 and 11, we estimate a value of 6.96 ± 0.09 eV for the IE of $Fe(CO)_4$. The dissociation energies for neutral $CO–Fe(CO)_n$, n = 0–3, are not well-known. Previous estimates[9,35,36,49] for these dissociation energies are listed in Table II to compare with D_0 values for $CO–Fe(CO)_n^+$, n = 0–4. Since these neutral bond dissociation energies have large uncertainties, the conversion of these values to 0 K is not made. The IE for $Fe(CO)_4$ and those for $Fe(CO)_n$, n = 1–3, estimated by using these values and the AEs for processes 3–5 are also included in Table II. The estimated values for IEs of $Fe(CO)_n$, n = 1–4, fall in the range of 7–7.9 eV. Since the IE of Fe differs substantially from that for CO, we expect that the bondings in these iron carbonyl compounds are weak and that their IEs are close to that of Fe.

The recent ab initio calculations[38] on the first- and second-row transition-metal mono- and dicarbonyl cations indicate that the bonding is dominated by electrostatic interaction and that the π-type bonding is weak in the iron mono- and dicarbonyl cations. Because of the electrostatic interaction, the D_0 values for $CO–FeCO^+$ and $Fe^+–CO$ should be greater than those for CO–FeCO and Fe–CO, a conclusion supported by experimental findings.[35,36]

D. Collision-Induced Dissociation Cross Sections for $FeCO^+$. Figure 6a,b shows the total absolute collision-induced dissociation cross sections for $FeCO^+$ prepared by process 5 at 900 and 790 Å, respectively. For reactant $FeCO^+$ ions formed at 790 Å, the cross section is found to increase linearly with increasing E_{lab}. The cross section has a value of about 2 $Å^2$ at E_{lab} = 0.2 eV. An E_{lab} value of 0.2 eV corresponds to a center-of-mass collision energy ($E_{c.m.}$) of 0.065 eV for this system. If the AE of 12.68 eV (978 Å) for the formation of $FeCO^+$ is the true threshold for reaction 5, $FeCO^+$ prepared at 790 Å may contain an internal energy ≤3.01 eV. The observation that the collision-induced dissociation remains relatively high at $E_{c.m.}$ close to zero is evidence that the bond dissociation energy for $Fe^+–CO$ is <3 eV. Assuming that the D_0 value for $Fe^+–CO$ is 39.3 kcal/mol as determined by the AE measurements and that excited $FeCO^+$ ions with internal energies greater than 39.3 kcal/mol dissociate rapidly in a time scale much shorter than the experimental time scale of about 40 μs, the internal energies for $FeCO^+$ prepared at 790 Å should be <1.7 eV (39.3 kcal/mol). In the case of $FeCO^+$ prepared at 900 Å, the cross section becomes essentially zero at $E_{c.m.}$ = 0.32 ± 0.16 eV (E_{lab} = 1 ± 0.5 eV). Considering that at 900 Å the internal energy for $FeCO^+$ may be equal to 1.10 ± 0.06 eV, we obtain an estimate of 1.42 ± 0.17 eV (33 ± 4 kcal/mol) for the D_0 value of $Fe^+–CO$. After taking into account the experimental uncer-

(43) Mittasch, A. *Angew. Chem.* **1928**, *41*, 827.
(44) *Selected Values of Chemical Thermodynamic Properties*; U.S. National Bureau of Standards Circular 500, U.S. Government Printing Office: Washington, DC, 1952.
(45) Cotton, F. A.; Fischer, A. K.; Wilkinson, G. *J. Am. Chem. Soc.* **1959**, *81*, 800.
(46) Moore, C. E. *Natl. Stand. Ref. Data Ser. (U.S. Natl. Bur. Stand.) NSRDS-NBS 34* **1970**.
(47) Gray, H. B.; Beach, N. A. *J. Am. Chem. Soc.* **1963**, *85*, 2922.
(48) Caulton, K. G.; Fenske, F. R. *Inorg. Chem.* **1968**, *7*, 1273.
(49) Engelking, P. C.; Lineberger, W. C. *J. Am. Chem. Soc.* **1979**, *101*, 5569.

tainties, the latter value is consistent with the D_0 value of 39.3 ± 2.0 kcal/mol for Fe^+–CO. The agreement found in the D_0 values for Fe^+–CO shows that the AE for reaction 5 determined in the PEPICO measurement is reliable.

IV. Conclusion

We have carried out a detailed study of processes 1–6 by using the PEPICO method. The bond dissociation energies for CO–$Fe(CO)_n^+$, n = 0–4, at 0 K are calculated by using the IE for $Fe(CO)_5$ and the AEs for the formation of $Fe(CO)_n^+$, n = 0–4. The D_0 value for Fe^+–CO thus determined by the PEPICO measurement is in accord with that obtained in the collision-induced dissociation study and the prediction of the recent ab initio calculation.

As the internal energy for $Fe(CO)_5^+$ is increased from 0 to 6.51 eV, the dissociation of $Fe(CO)_5^+$ may take place by sequential loss of CO. In the internal energy range of 6.51–8.65 eV, the PEPICO intensities for $Fe(CO)_2^+$, $FeCO^+$, and Fe^+ are finite, indicating that $Fe(CO)_2^+$ may dissociate directly to both $FeCO^+$ and Fe^+.

Acknowledgment. The authors are grateful to Prof. R. J. Angelici for his encouragement and interest in this project. C.Y.N. thanks Dr. L. A. Barnes for a helpful discussion.

Transition Structures for Hydrogen Atom Transfers to Oxygen. Comparisons of Intermolecular and Intramolecular Processes and Open- and Closed-Shell Systems

Andrea E. Dorigo, Margaret A. McCarrick, Richard J. Loncharich, and K. N. Houk*

Contribution from the Department of Chemistry and Biochemistry, University of California, Los Angeles, Los Angeles, California 90024-1569. *Received January 9, 1989*

Abstract: The transition structures for the intramolecular hydrogen atom abstractions of the butoxy radical, the triplet and the radical cation states of butanal, and the radical cation of butanol, as well as that of the thermal retro-ene reaction of butanal, were located with ab initio molecular orbital calculations. These processes are the rate- and/or product-determining steps in common reactions like the Barton reaction, the Norrish type II photochemical reaction, and the McLafferty rearrangement of radical cations in mass spectrometry. The corresponding intermolecular hydrogen abstractions from methane by the methoxy radical, triplet formaldehyde, formaldehyde radical cation, and the methanol radical cation were located for comparison, using UHF theory and correlation theory corrections at the MP2 level. Differences in activation energy are related to the electronic differences between closed-shell, open-shell, and charged open-shell systems. Regioselective hydrogen atom transfer in the Norrish type II reaction is due to a combined enthalpic and entropic preference for a six-membered-ring transition structure. Our calculations indicate a strong preference for in-plane hydrogen abstraction by triplet aldehydes.

Introduction

Hydrogen atom transfers are ubiquitous reactions in organic chemistry. These reactions have many features in common with proton transfers, events that are of fundamental importance in most branches of chemistry. There have been a number of quantitative theoretical treatments of hydrogen atom transfers, starting with early investigations of the reaction between a hydrogen atom and a hydrogen molecule.[1] In recent times, theoretical treatments have been applied to more complex systems.[2] The most commonly studied type of hydrogen atom transfer involves the abstraction of an alkyl hydrogen by an oxygen species having an unpaired electron.[3] *Intramolecular* hydrogen atom abstractions by various reactive oxygen functionalities generally involve six-membered-ring transition states and are often accompanied or followed by skeletal rearrangements or fragmentation. Until recently, high-level quantum chemical calculations on the systems in question were not practical. Recently, several semiempirical calculations have been reported for the McLafferty rearrangement and the Norrish type II reaction,[4-6] and one ab initio calculation has been reported on the McLafferty rearrangement.[7]

We have undertaken ab initio molecular orbital computational studies of the most important processes (see Scheme I) of this kind in solution and in the gas phase: (1) the Barton reaction,[8] (2) the Norrish type II cleavage,[9] (3) the McLafferty rearrangement,[10] and (4) the related reactions of alcohol and ether radical cations.[10,11] The analogous reaction of a closed-shell species is the retro-ene reaction of carbonyl compounds (5).[12] This paper describes the results of our calculations on these processes and on the related intermolecular reactions. We are in the process of developing force fields for these processes similar to that we have reported for reaction 1.[13,14] Our calculations were designed

(1) London, F. Z. *Elektrochem.* **1929**, *35*, 552. Barker, R. S.; Snow, R. L.; Eyring, H. *J. Chem. Phys.* **1955**, *23*, 1686.
(2) Some examples include: (a) $H^\bullet + CH_4$: Morokuma, K.; Davis, R. E. *J. Am. Chem. Soc.* **1972**, *94*, 1060. (b) $^3O + H_2$: Walch, S. P.; Dunning, T. H., Jr. *J. Chem. Phys.* **1980**, *72*, 406. (c) $HO^\bullet + H_2$: Walch, S. P.; Dunning, T. H., Jr. *J. Chem. Phys.* **1980**, *72*, 1303. See also ref 23. (d) $HO^\bullet + CH_4$: Gordon, M. S.; Truhlar, D. G. *J. Am. Chem. Soc.* **1986**, *108*, 5412.
(3) Wilt, J. W. In *Free Radicals*; John Wiley & Sons: New York, 1973; Vol. I, p 378.
(4) Boer, F. F.; Shannon, T. W.; McLafferty, F. W. *J. Am. Chem. Soc.* **1968**, *90*, 7239.
(5) Dewar, M. J. S.; Doubleday, C. *J. Am. Chem. Soc.* **1977**, *99*, 4935.
(6) Dougherty, R. C. *J. Am. Chem. Soc.* **1968**, *90*, 5780.
(7) Ha, T.-K.; Radloff, C.; Nguyen, M. T. *J. Phys. Chem.* **1986**, *90*, 2991.
(8) (a) Barton, D. H. R.; Beaton, J. M.; Geller, L. E.; Pechet, M. M. *J. Am. Chem. Soc.* **1960**, *82*, 2640. (b) Barton, D. H. R.; Beaton, J. M. *Ibid.* **1960**, *82*, 2641. (c) Walling, C.; Padwa, A. *J. Am. Chem. Soc.* **1963**, *85*, 1593. (d) Brun, P.; Waegell, B. In *Reactive Intermediates*; Plenum Press: New York, 1983; Vol. 3, p 367 and references therein.
(9) (a) Wagner, P. J.; Kelso, P. A.; Kemppainen, A. E.; Zepp, R. G. *J. Am. Chem. Soc.* **1972**, *94*, 7500. (b) Wagner, P. J. *Acc. Chem. Res.* **1971**, *4*, 168.
(10) (a) Seibl, J.; Gäumann, T. *Helv. Chim. Acta* **1963**, *46*, 2857. (b) Arndt, R. R.; Djerassi, C. *Chem. Commun.* **1965**, 518. (c) Kingston, D. G. I.; Bursey, J. T.; Bursey, M. M. *Chem. Rev.* **1974**, *74*, 215 and references cited therein. (d) Budzikiewiz, H.; Djerassi, C.; Williams, D. H. *Mass Spectrometry of Organic Compounds*; Holden-Day Inc.: San Francisco, CA, 1967.
(11) Biermann, H. W.; Morton, T. H. *J. Am. Chem. Soc.* **1983**, *105*, 5025 and refrences therein.
(12) (a) The intramolecular reaction between an enol and an alkene proceeds thermally at temperatures of about 350 °C. For a review see: Conia, J. M.; Le Perchec, P. *Synthesis* **1975**, 1. (b) For calculations on related ene reactions, see: Loncharich, R. J.; Houk, K. N. *J. Am. Chem. Soc.* **1987**, *109*, 6947.
(13) Dorigo, A. E.; Houk, K. N. *J. Org. Chem.* **1988**, *53*, 1650.
(14) Dorigo, A. E.; Houk, K. N. *J. Am. Chem. Soc.* **1987**, *109*, 2195–2197.

0002-7863/90/1512-7508$02.50/0